Pten Deletion in Adult Neural Stem/Progenitor Cells Enhances Constitutive Neurogenesis

Caroline Gregorian[1], **Jonathan Nakashima**[1], **Janel Le Belle**[1], **John Ohab**[2], **Rachel Kim**[1], **Annie Liu**[1], **Kate Barzan Smith**[1], **Matthias Groszer**[1,3,5], **A. Denise Garcia**[4], **Michael V. Sofroniew**[4], **S. Thomas Carmichael**[2], **Harley I. Kornblum**[1,6], **Xin Liu**[1,3], and **Hong Wu**[1,*]

[1]Department of Molecular and Medical Pharmacology, David Geffen School of Medicine, University of California, Los Angeles, CA 90095, USA

[2]Department of Neurology, David Geffen School of Medicine, University of California, Los Angeles, CA 90095, USA

[3]Department of Pathology and Laboratory Medicine, David Geffen School of Medicine, University of California, Los Angeles, CA 90095, USA

[4]Department of Neurobiology, David Geffen School of Medicine, University of California, Los Angeles, CA 90095, USA

[6]The Semel Institute, David Geffen School of Medicine, University of California, Los Angeles, CA 90095, USA

Abstract

Here we show that conditional deletion of PTEN in a subpopulation of adult neural stem cells in the subependymal zone (SEZ) leads to persistently enhanced neural stem cell self-renewal without sign of exhaustion. These *Pten* null SEZ-born neural stem cells and progenies can follow the endogenous migration, differentiation, and integration pathways and contribute to the constitutive neurogenesis in the olfactory bulb. As a result, the *Pten* deleted animals have increased olfactory bulb mass and enhanced olfactory function. *Pten* null cells in the olfactory bulb can establish normal connections with peripheral olfactory epithelium and help olfactory bulb recovery from acute damage. Following a focal stroke, *Pten* null progenitors give rise to greater numbers of neuroblasts that migrate to peri-infarct cortex. However, contrary to olfactory bulb, no significant long-term survival and integration can be observed, indicating that additional factors are necessary for long-term survival of newly born neurons after stroke. These data suggest that manipulating PTEN-controlled signaling pathways may be a useful step in facilitating endogenous neural stem/progenitor expansion for the treatment of disorders or lesions in regions associated with constitutive neurogenesis.

Keywords

SEZ; PTEN; neurogenesis; olfactory; neural repair; post-stroke

INTRODUCTION

The adult central nervous system contains self-renewing stem cells capable of generating new neurons, astrocytes, and oligodendrocytes, a process evolutionarily conserved in birds, rodents,

Corresponding Author: Dr. Hong Wu, Department of Molecular and Medical Pharmacology, CHS 23-214, UCLA School of Medicine, 650 CE Young Drive South, Los Angeles, CA 90095-1735, 310-825-5160 (office), 310-267-0242 (fax), hwu@mednet.ucla.edu.
[5]Present address: Wellcome Trust Centre for Human Genetics, University of Oxford, Roosevelt Drive, Oxford, UK.

primates, and humans (Doetsch, 2003). The subependymal zone (SEZ) is one of at least two areas of adult neurogenesis where glial fibrillary acidic protein (GFAP) expressing cells act as slow-dividing neural stem cells (NSCs) capable of generating neuroblast precursors (Doetsch, 2003; Garcia et al., 2004; Lledo et al., 2006). The neuroblasts migrate into the rostral migratory stream (RMS) and then into the olfactory bulb (OB) where they differentiate into granule and periglomerular neurons (Curtis et al., 2007; Hack et al., 2005; Lois et al., 1996; Luskin, 1993; Petreanu and Alvarez-Buylla, 2002). Since the majority of granule neurons in the OB are generated postnatally (Petreanu and Alvarez-Buylla, 2002), it is believed that continued neoneurogenesis from the SEZ is critical for maintaining the homeostasis of the OB and therefore the olfactory functions (Goldman, 1998).

NSC-mediated neoneurogenesis is also believed to participate in the process of neural repair. Recent findings suggest endogenously generated new neurons participate in the formation of circuitry and at least some functional recovery following neurological damage such as stroke (Yamashita et al., 2006). Therefore, understanding the molecular mechanisms and pathways capable of activating and expanding neural stem/precursor cell (NS/PC) populations, stimulating their migration toward damaged or diseased areas, enhancing their survival, and promoting their maturation and integration into the existing neural circuitries may ultimately lead to repair and improve damaged neuronal functions (Emsley et al., 2005; Peterson, 2002).

Phosphatase and tensin homologue deleted on chromosome 10 (*PTEN*) encodes a phosphatase and is a potent antagonizer of phosphatidylinositol-3-kinase (PI3K) (Li et al., 1998; Liaw et al., 1997; Nelen et al., 1997) and its regulated pathways (Lee et al., 1999; Maehama et al., 2001; Vivanco and Sawyers, 2002). Utilizing Cre-Lox technology, our group as well as others have generated mouse models with conditional deletion of the murine homolog of the *PTEN* gene (*Pten*) in the brain at different developmental stages (Backman et al., 2001; Fraser et al., 2004; Groszer et al., 2001; Kwon et al., 2001; Marino et al., 2002; Stiles et al., 2004; Yue et al., 2005). By deleting *Pten* in the embryonic NSCs, we showed PTEN negatively regulates NSC proliferation, survival, and self-renewal, both *in vivo* and *in vitro* (Groszer et al., 2006; Groszer et al., 2001). Our recent results demonstrate that *Pten* null NS/PCs have enhanced self-renewal capacity, accelerated G0-G1 cell cycle entry, shortened cell cycle, and decreased growth factor dependency (Groszer et al., 2006). Therefore, loss of PTEN is sufficient to increase the pool of self-renewing NSCs and promote their escape from the homeostatic mechanisms of proliferation control while cell fate commitments of the *Pten* null NS/PCs are largely undisturbed (Groszer et al., 2006; Groszer et al., 2001).

Because PTEN loss can lead to enhanced embryonic NSC self-renewal, proliferation, and survival, its transient inactivation may be a promising approach for "boosting" the limited adult NSC population, a critical step towards treating certain neurodegenerative diseases. However, such an approach would have to be vigorously tested *in vivo* to ensure 1) that the PTEN-PI3K pathway plays a similar role in adult NSCs, and 2) perturbation of PTEN-PI3K pathway alone in NSCs is not tumorigenic. To address these issues and further explore the role of PTEN in regulating adult neurogenesis and repair *in vivo*, we deleted PTEN in a subpopulation of adult NS/PCs in the SEZ by crossing *Pten* conditional knockout mice (*Pten^{loxp/loxp}*) (Lesche et al., 2002) with a murine *GFAP-Cre^+* (*mGFAP-Cre^+*) transgenic line.

MATERIALS AND METHODS

Animals

mGFAP-Cre^+ transgenic mice line 77.6 were generated using a 15-kb promoter cassette containing the full length sequence of the murine GFAP gene as described previously for line 73.12 (Garcia et al., 2004) and crossed to *Pten^{loxp/loxp}* mice (Lesche et al., 2002) on a 129/Balb/c background. F_1 generation compound heterozygous animals were backcrossed with

$Pten^{loxp/loxp}$ mice to produce F2 generation experimental animals. Animals were genotyped by standard genomic PCR techniques (Lesche et al., 2002). $Pten^{loxp/loxp}$;*mGFAP-Cre*$^+$ mice were crossed to ROSA26 mice (Soriano, 1999) for reporter analysis. In addition to the SEZ, 77.6 mice exhibited only a scattered mosaic pattern of Cre/β-gal expression in subpopulations of GFAP$^+$ astrocytes in the adult brain. Animals were housed in a temperature-, humidity-, and light-controlled room (12-h light/dark cycle), and allowed free access to food and water. All experiments were conducted according to the research guidelines of the UCLA Chancellor's Animal Research Committee.

Polymerase Chain Reaction (PCR)

The specificity of *Pten* excision was evaluated by PCR using DNA from tail clip biopsy. For *Pten* PCR, the loxp (650 bp), wild-type (500 bp), and exon 5 (300 bp) fragments are amplified simultaneously by using three primers TCCCAGAGTTCATACCAGGA (Pten6637-F), GCAATGGCCAGTACTAGTGA-AC (Pten6925-R), and AATCTGTGCATGAAGGGAAC (Pten7319-R). PCR was performed in 20 µl reactions using standard procedures for forty cycles; each cycle consisted of denaturing at 94°C for 45", annealing at 60°C for 30", and extension at 72°C for 1', followed by a single 5' extension at 72°C. The PCR products were analyzed on 2% agarose gels.

5-Bromo-2′-Deoxyuridine (BrdU) Labeling

BrdU (Sigma, B5002) was given as either a single i.p. injection of 200 mg/kg followed by perfusion with 4% paraformaldehyde after 2 h, or as four i.p. injections of 200 mg/kg every 12 h followed by perfusion after 14 d. Staining with anti-BrdU antibody (1:1000 BD Biosciences, 51–75512) was performed according to manufacturer's suggestions.

Neurosphere Cultures

Neurosphere cultures were prepared as described previously (Groszer et al., 2006). Briefly, 8 week old SEZs were dissected, minced with a razor blade, dissociated by enzymatic digestion with Accumax followed by light trituration with a fire-polished glass pipette, and passed through a 70 µM nylon mesh. For moderate density cultures, cells were re-suspended at 10,000 cells/ml (10K) in Neurobasal medium (Gibco), supplemented with B-27 (Gibco), Heparin (Sigma), 20 ng/ml basic fibroblast growth factor (bFGF, Peprotech), and 20 ng/ml epidermal growth factor (EGF, Invitrogen). For clonal/low density cultures, tertiary neurospheres were dissociated into a single cell suspension as described above and the cells were plated at 1,000 cells/ml (1K) in T25 tissue culture flasks. Clonal cultures were passaged every two weeks. At passage 1, 4, 8, 16 and 24 cells were also plated into 96 well plates at clonal density and after 10 days clonal neurospheres were counted and differentiated All neurospheres in the 96-well clonal plates which measured greater than 40uM in diameter were counted using the Microcomputer Imaging Device Program (MCID).

Immunocytochemistry of Neurospheres

Immunocytochemistry of neurosphere cultures was performed as described previously (Groszer et al., 2001). Breifly, following neurosphere counting, at least 20 randomly chosen clonal neurospheres were transfered from the 96-well plates onto Poly-l-lysine (BD Biosciences) and laminin-coated glass coverslips (one sphere per coverslip) for differentiation in Neurobasal medium in the absence of growth factors. After five days, the differentiated neurospheres were fixed in 4% paraformaldehyde and immunostained with rabbit anti-Tuj1 (1: 1000; Covance, MMS-435P); for neurons, **α** GFAP (DAKO) for astrocytes, and **α** O4 (Chemicon) for oligodendrocytes.

Image Analysis and Quantification

BrdU-immunostained (BrdU[+]) nuclei were visualized with a Leica light microscope (40X objective) equipped with a charge-coupled device digital camera. For 14 d post-injection, comparable sections of immunostained profiles contained in the GCL and RMS were counted in 5 µm thick serial sections at 100 µm intervals. For the 2 h post-injection period, the numbers of BrdU[+] nuclei were counted in coronal sections of SEZ and OB. The respective areas of these layers/regions were determined with SIMPLE PCI software and the quantified values were converted to densities (number of BrdU[+] profiles per mm^2) n=6. The structure volumes and RMS were measured as described previously (Petreanu and Alvarez-Buylla, 2002; Tsai et al., 2006).

Histology and Immunohistochemistry of Tissue Sections

All IHC staining was performed on 5 µm sections that were prepared from paraffin-embedded blocks and placed on charged glass slides. The slides were deparaffinized with xylene and rehydrated in descending grades (100%–70%) of ethanol. The endogenous peroxidase activity was inactivated in 3% hydrogen peroxide (H_2O_2). After washing in deionized water, antigen retrieval was performed by incubating the slides in 0.01 M citric acid buffer (pH 6.0) at 95°C for 13.5 min. Slides were then allowed to cool for 30 min in citric acid buffer. After washing in deionized water, the slides were transferred to either PBS (pH 7.4) or TBST for 5 min. For DAB staining, slides were first blocked with 5% normal goat serum then incubated with primary antibody overnight at 4°C. Following three 5 min washes in either PBS or TBST, slides were incubated with biotinylated secondary antibody (1:200, Biogenex) for 30 min at room temperature. Amplification was performed with a horseradish peroxidase system (Vectastain ABC kit, Vector, PK-6100) using a liquid DAB peroxidase substrate (Biogenex, HK130-5K). Slides were counterstained in Gill's hematoxylin, dehydrated, cleared, and cover-slipped. Negative control slides were run without primary antibody. For fluorescence double staining, the section was treated as above and first stained with the first antibody followed by signal amplification with TSA Plus Fluorescence Systems (PerkinElmer, NEL-7448). After biotin blocking, the section was stained with the second antibody and signal was amplified with TSA system with different fluorescence. Primary antibodies used were rabbit anti-PTEN (1:100, Cell Signaling 9552); rat anti-GFAP (1:1000, ZYMED Laboratories, 18-0063); goat anti-Nestin (1:50; R&D Systems, AF2736); rabbit anti-Cre (1:3000; Covance PRB-106C); goat antidoublecortin (1:500; Santa Cruz, sc8066); mouse anti-NeuN (1:1000; Chemicon, MAB377); rabbit anti-β-galactosidase (1:1000; MP Biochemicals, 55976); rabbit anti-ki-67 (1:100; Vector, VP-RM04). 4′,6-diamidino-2-phenylindole (DAPI; Molecular Probes, D-1306) used as a fluorescent counterstain.

Olfactory Habituation Test

This task measured the ability of mice to detect a novel odorant and to habituate responding to that odorant over repeated presentations. Previous studies (Trinh and Storm, 2004) demonstrated that a high number of sniffs upon initial exposure of an odorant indicated that the animal detected a novel odorant. Each mouse was housed individually and handled daily for five days prior to the beginning of any behavioral manipulation. Individual mice were then exposed to an odorant for three successive 2-min trials separated by 1-min intervals. The first odorant was always sterile water in order to habituate the animal to the introduction of a novel object (cotton swab) in the home cage. Following this pre-exposure phase, a cotton swab saturated with an odorant was introduced into the home cage for another three successive 2-min trial separated by 1-min intervals. The total number of contacts that the mouse made with the cotton swab for each of three two-minute exposures as well as the total amount of time spent in contact with the cotton swab was recorded. The odorants used were isoamyl acetate, isomenthone, hexyl alcohol, limonene, and anisole (Sigma). For data collection and analysis,

all experiments were recorded using a camcorder. The number of sniffs and the duration of each sniff were analyzed in a blind setting by viewing recordings in real time. In order to be consistent and unbiased in analysis, a full sheet of plain paper with a 1 in^2 box was cut out and placed onto the screen with the cotton swab directly in the middle of the box, thus blocking the rest of the screen. Every time the nose of the mouse entered the box, it was scored as a sniff; the duration of each sniff was recorded as the amount of time the nose of the mouse remained in the box. Time intervals were divided into five categories of time as follows: less then 1, 2–5, 6–9, 10–12, and more than 12 seconds. A total of 14 control (*Pten$^{loxp/loxp}$*) and 12 mutant (*Pten$^{loxp/loxp}$;mGFAP-Cre$^+$*) sexually naïve male mice at 10–12 months of age were used in behavior experiments.

Chemical Ablation of Olfactory Epithelium

Eight control (*Pten$^{loxp/loxp}$*) and 8 mutant (*Pten$^{loxp/loxp}$;mGFAP-Cre$^+$*) sexually naïve 14–16 week old male mice were housed individually and given i.p. injections of dichlobenil (2.6-dichlobenzonitrile, Sigma, 25 µg/g body weight) in DMSO (dimethyl sulphoxide, 2 µl/g body weight) for 7 days (Yoon et al., 2005). 5 control (*Pten$^{loxp/loxp}$*) and 5 mutant (*Pten$^{loxp/loxp}$;mGFAP-Cre$^+$*) were given DMSO (2 µl/g body weight). All mice were evaluated for ability to detect novel odors using the odorant habituation test at 2, 3, and 4 weeks1, and 28 days after the last injection.

Stroke Model

Stroke was produced in 2–5 month old *Pten$^{loxp/loxp}$;mGFAP-Cre$^+$* and control animals as described previously (Carmichael, 2005; Tsai et al., 2006).

Stereology

Stereological quantification was performed using serial sections through the anterior SEZ, OB, and peri-infarct cortex using unbiased counting with the optical fractionator as described previously (Tsai et al., 2006).

Infarct Volume

Infarct volume was measured 7 d after stroke in *Pten$^{loxp/loxp}$;mGFAP-Cre$^+$* and control mice (n=5) as described previously (Tsai et al., 2006).

Statistical Analysis

All data were subjected to statistical analysis by using two-sample *t* testing assuming unequal variances (Excel Data Analysis Tool Pak, Microsoft) to determine the differences between the control and mutant groups. A *P* value of 0.05 or less was considered significant and symbolized as single asterisk (*), a *P* value of 0.01 or less as double asterisks (**), and a *P* value of 0.001 or less as triple asterisks (***). A *P* value greater than 0.05 was not considered significant.

RESULTS

Generation of *mGFAP-Cre$^+$* Line for Conditionally Targeting Adult Neural Stem/Progenitor Cells

Previous studies have made a compelling case that the majority of multipotent NSCs responsible for neoneurogenesis in the adult mouse brain express GFAP (Doetsch et al., 1999; Garcia et al., 2004; Groszer et al., 2001; Imura et al., 2003). To further explore the role of PTEN in regulating adult neurogenesis and repair *in vivo*, we generated a new *mGFAP-Cre$^+$* transgenic line 77.6 using the *mGFAP* gene cassette (Garcia et al., 2004) (for details, please see Experimental Procedures). Immunohistochemistry (IHC) *of 77.6* mice crossed to *Rosa26-LacZ* reporter mice (Soriano, 1999) showed Cre expression in a small subpopulation

of SEZ cell in adult brain (Figure 1A and 1B) and β-Gal expression in many more cells corresponding to Cre$^+$ cells and their progenies (Figure 1E). These Cre$^+$/β-Gal$^+$ cells represent adult NSCs since their progenies can migrate and differentiate along the RMS (Figure 1F) and reach the granule cell layer (GCL) in the OB (Figure 1H). In addition, we used double-labeling immunohistochemistry to compare expression of Cre with GFAP and Nestin, intermediate filaments whose dynamic regulation by neural progenitors and astrocytes at different stages of development has been well documented (Garcia et al., 2004; Lagace et al 2007). Three dimensional analysis of SEZ cells using scanning confocal laser microscopy showed that Cre + cells in the SEZ express GFAP (Figure 1C) and Nestin (Figure 1D). Cells that were Cre positive/GFAP negative or Cre positive/Nestin negative were not found (data not shown). Furthermore, neither Cre nor LacZ reporter expression could be detected in embryonic brains (data not shown), suggesting Cre is not expressed during embryonic development, and only postnatally in progenitor cells. In contrast to the previously reported *mGFAP* lines 7.1 (Bush et al., 1998; Imura et al., 2003) and 73.12 (Garcia et al., 2004), *mGFAP-Cre$^+$* line 77.6-mediated reporter expression in progenitor cells was limited to the SEZ region and no Cre or LacZ reporter expression could be detected in GFAP$^+$ NSC populations in the hippocampus. Therefore, *mGFAP-Cre$^+$* line 77.6 was chosen for this study because we hypothesized that the limited Cre transgene expression in NSCs of line 77.6 would circumvent increased brain size, altered brain histoarchitecture and premature lethality caused by global *Pten* deletion from NSCs in previous conditional knockout models (Groszer et al., 2001; Yue et al., 2005).

PTEN Deletion in the Adult NSC Leads to Increased Self-Renewal without Tumorigenesis or Premature Senescence

To explore PTEN's role in regulating adult NSCs, *Pten$^{loxp/loxp}$* (Lesche et al., 2002) mice were crossed with *mGFAP-Cre$^+$* line 77.6 mice. *Pten$^{loxp/loxp}$;mGFAP-Cre$^+$* mutants are viable and fertile, yielding Mendelian offspring distributions (data not shown). Importantly, no tumors or aberrant neurological phenotypes were detected in mutant animals up to two years of age.

Previously, we found that deletion of PTEN in embryonic NSC resulted in an enhanced ability to self-renew in vitro with a greater capacity to produce neurons over time in culture as compared to control spheres (Groszer et al., 2006). To assess the function of PTEN in controlling adult NSC self-renewal and proliferation, we compared neurosphere forming activity of *Pten* deleted brain (Mutant) with that of their wild-type littermates (Control) in a serial clonal passaging experiment. Similar to *Pten* deletion in the embryonic neural stem cells, spheres formed from *Pten* deleted adult brain were generally bigger (Supplementary Figure 1A). Importantly, by passage 4 over 90% of spheres isolated from the mutant cultures carried *Pten* biallele deletion and were positive for the Cre transgene (Supplementary Figure 1B). At each passage, *mGFAP-Cre*-mediated *Pten* deletion in adult NSCs resulted in increased clonal neurosphere number, a measurement of neural stem cell self-renewal capacity (Figure 2A). Serial clonal passaging of cells over 48 weeks (24 passages), at a density at which nearly all spheres are derived from a single cell, resulted in the eventual senescence of wild-type cultures whilst the mutant cells maintained high rates of self-renewal. This enhanced neurosphere formation was also reflected in the total cell numbers attained at each passage (Figure 2B). Following *in vitro* differentiation, the clonal neurospheres from mutant mice maintained a significantly enhanced neurogenesis even at late passages, whereas the wild-type cultures produced fewer neurons than their mutant counterpart at every passage and their ability to generate neurons declined substantially with time in culture (Figure 2C), similar to our previous studies on *Pten* deleted embryonic NSCs (Groszer et al., 2001). Taken together, these data indicate that *Pten* deletion persistently enhances self-renewal of adult NSC, while maintaining their capacity to produce neurons, without any evidence of stem cell exhaustion.

Pten Deletion leads to Expansion of Neural Stem and Progenitor Cells in the SEZ Region

At the tissue level, *Pten* deletion led to a robust increase in GFAP^{+} cells (Figure 3A) in the SEZ. Cells with hyperphosphorylation of S6 (P-S6, Figure 3A) and AKT (P-AKT, Supplementary Figure 2A), surrogate markers for PTEN loss and PI3K activation that have been implicated in neuron survival and cell cycle control (Datta et al., 1999), could be easily visualized in the same region. GFAP expression and numbers of GFAP^{+} cells did not appear different from controls in neighboring structures and other parts of forebrain except the SEZ region (data not shown), further supporting SEZ-specific *Pten* deletion. Importantly, these P-S6^{+} cells also express GFAP (Figure 3A) and/or Doublecortin (DCX), a marker for immature and migrating neuroblast progenitors (Supplementary Figure 2B), suggesting that PTEN loss or PI3K-AKT activation leads to the expansion of adult NSC and progenitors in SEZ region.

Consistent with NSC expansion, the volume of the mutant SEZ is significantly increased when compared to controls (Figure 3B, 0.021 ± 0.0011 vs. 0.032 ± 0.008 mm^3 $\pm$ SEM; p<0.05), which was accompanied by a greater number of Ki-67^{+} (Figure 3C; 6832.12 ± 231.8 vs. 8376.98 ± 122.8 cells $\pm$ SEM; P<0.05) and DCX[+] neuroblasts (Feng and Walsh, 2001). Figure 3D shows a statistically significant (p<0.01) increased DCX volume in *Pten^{loxp/loxp}*;*mGFAP-Cre^{+}* SEZ (Figure 3D, 0.019 ± 0.0012 vs. 0.062 ± 0.0064 mm^3 $\pm$ SEM). These results indicated that *Pten* null NSCs can readily proliferate and differentiate into DCX[+] neuroblasts, the precursors for adult neurogenesis.

SEZ-Born *Pten* Null Progenitors and Their Progenies Follow the Endogenous Migration Pathway

SEZ-born progenitors are known to migrate to the OB via the well-defined RMS. Because PTEN has been implicated in controlling cell chemotaxis (Funamoto et al., 2002; Iijima and Devreotes, 2002) as well as migration (Liliental et al., 2000; Raftopoulou et al., 2004; Tamura et al., 1998; Yue et al., 2005), we determined whether the progenies of SEZ-born *Pten* null progenitors could respond to normal environmental cues and migrate into and along the RMS. To mark the SEZ-born progenitors and their differentiated progenies, we pulse labeled control and mutant mice with BrdU and quantified the number of BrdU^{+} cells in the RMS after 5 days of chase. As shown in Figure 4A, a significant increase in the number of BrdU^{+} cells was found in the mutant RMS (Figure 4A, 1485.34 ± 182.32 vs. 2697 ± 324.20 cells per mm^2 $\pm$ SEM; p<0.001). Furthermore, the BrdU^{+} cells were also positive for P-S6 staining (Figure 4B), indicating that SEZ-born *Pten* null progenitors exhibited enhanced cell proliferation and could follow the endogenous migration pathway into the RMS.

We then tested whether the migrating *Pten* null progenitors within the RMS express similar markers as controls. Neuroblasts in mutant RMS are *Pten^{−}* (Supplementary Figure 3) and DCX[+] (Figure 4C) with many more DCX[+] neuroblasts in the RMS of *Pten^{loxp/loxp}*;*mGFAP-Cre^{+}* mice (Figure 4D; 2642 ± 126 vs. 3894 ± 60 cells per mm^2 $\pm$ SEM; p<0.05).

During migration, neuroblasts are restricted to the RMS with few cells diverging from the path (Doetsch and Alvarez-Buylla, 1996). Although it seemed that a greater number of cells diverged from the RMS in the *Pten^{loxp/loxp}*;*mGFAP-Cre^{+}* mice, the ratio of diverging DCX^{+} cells to the total number of cells in the mutant RMS was not significantly different from that of controls (Figure 4E, 1.28 ± 0.004 vs. $1.36 \pm 0.009\%$ of total $\pm$ SEM; p>0.05). These results suggest that *Pten* null SEZ-born neuroblasts are able to recognize environmental cues and migrate along the endogenous pathway.

Deletion of PTEN in Adult SEZ Leads to Increased OB Mass

Although OB granule cell neurons (GC) are continuously generated throughout adulthood, OB volume remains constant during adulthood (Pomeroy et al., 1990). This homeostatic stage is

achieved largely via a balance between SEZ neoneurogenesis and cell death in the GCL of OB (Fiske and Brunjes, 2001; Najbauer and Leon, 1995; Petreanu and Alvarez-Buylla, 2002). Measurements taken from mutants and their littermate controls demonstrated continuous increases in size (Figure 5A, left panel) and weight of mutant OB, starting at 2.5 months of age (Figure 5A, right panel). This increased size and mass of mutant OB is consistent with previous reports that there is a surge of progenitors migrating to the OB at 3–4 months of age (Petreanu and Alvarez-Buylla, 2002). Histological analysis of mutant OB (Figure 5B) and other brain regions (Supplementary Figure 4) revealed normal histoarchitecture.

Because SEZ-born progenitors migrate and integrate into the GCL of the OB, we hypothesized that an increase in GCL volume may contribute to the increased OB mass. Compared to control, $Pten^{loxp/loxp}$;mGFAP-Cre$^+$. GCL volume increased 2 fold at 3.5 months (Figure 5C, columns on the left; 2.92 ± 0.071 vs. 5.60 ± 0.25 mm$^3 \pm$ SEM; p<0.05) while no statistically significant differences were observed in the external plexiform layer (EPL) (Figure 5C, columns on the right; 1.19 ± 0.054 vs 1.10 ± 0.043 mm$^3 \pm$ SEM; p<0.05), a region not influenced by SEZ-mediated neurogenesis. To further test whether increased GCL volume is due to SEZ-born granule cells incorporated into the OB, mice were injected with BrdU and sacrificed at 2 hr or 14 days after the last injection. These time points were chosen to ensure that there were no ectopic proliferating cells in the mutant OB (2 hr chase) and to allow sufficient time for BrdU-labeled neuroblasts to migrate, differentiate, and incorporate into the outer layers of the OB (14 day chase). BrdU$^+$ cells could not be detected in either control or mutant OB after 2 hrs of chase (Supplementary Figure 5). However, after 14 day chase there was an approximate 2-fold increase in the number of BrdU$^+$ cells in the GCL of 3.5 month old $Pten^{loxp/loxp}$;mGFAP-Cre$^+$ mice when compared to wild-type controls (Figure 5D; 2.92 ± 0.07 vs. 5.60 ± 0.25 cells $\pm$ SEM; p<0.001). These results indicate that the increase in GCL volume was not due to ectopic cell proliferation within the OB but from an increase in the number of cells that migrated from the SEZ to the GCL via the RMS. We also observed a significant decrease in the number of TUNEL$^+$ cells in the GCL (Figure 5E; 2.51 ± 0.22 vs. 1.83 ± 0.16 cells $\pm$ SEM; p<0.05), indicating that OB enlargement in the mutant mice is a net result of increased cell proliferation and decreased cell death. Furthermore, $Pten$ null NSC-derived granule neurons in the GCL were positive for both P-S6 and NeuN, a neuron-specific marker (Figure 5F). Taken together, these results indicate that $Pten$ deleted NSCs and their progenies can follow endogenous cues along the normal RMS and reach the OB. Within the OB, they can differentiate and integrate into the GCL.

$Pten^{loxp/loxp}$;mGFAP-Cre$^+$ Mice Exhibit Enhanced Habituation to Novel Odors

The life-long neurogenesis along SEZ-RMS-OB suggests that adult-born neurons play critical roles in olfactory functions (Petreanu and Alvarez-Buylla, 2002; Winner et al., 2002): adult-born neurons extend new processes and form new synapses with each other or with existing GC (Cecchi et al., 2001; Petreanu and Alvarez-Buylla, 2002), and the rates of neurogenesis are known to be positively correlated with performance on memory (Nilsson et al., 1999; Rochefort et al., 2002; Shors et al., 2001) and olfactory discrimination tasks (Enwere et al., 2004; Gheusi et al., 2000). To test whether SEZ-derived $Pten$ null GCs are functional, we performed an olfactory behavioral test. This Odorant Habituation Task behavioral assay measures the ability of mice to detect a novel odorant and to habituate in responding to that odorant over repeated presentations (Trinh and Storm, 2004). We found that olfactory discrimination was intact in $Pten^{loxp/loxp}$;mGFAP-Cre$^+$ mice since the first exposure to an odorant resulted in an increase in the number of sniffs from the previous trial, proving that the mice were able to detect a novel odor (Figure 6A). Furthermore, mutant mice habituate faster to a novel odorant when compared to controls, as demonstrated by a decrease in the number of sniffs during the second and third exposures of both isoamyl acetate and isomenthone (Figure 6A, right panels). A similar pattern was observed with two additional odorants regardless of

order of presentation (data not shown). In addition, when the duration of the sniffs was measured, $Pten^{loxp/loxp}$;$mGFAP$-Cre^+ mice exhibited a decrease in the time spent within each odorant group in comparison to controls (Supplementary Figure 6). A decrease in the time spent investigating an odorant after repeating exposure further implies that $Pten^{loxp/loxp}$;$mGFAP$-Cre^+ mice have an increased ability to recall, recognize, or habituate to the odorant when compared to control.

This enhanced odorant habituation suggests that 1) $Pten$ deletion in adult NSC causes enhanced proliferation and self-renewal without interfering with the normal properties and destiny of their differentiated progenies, and 2) $Pten$ null granule neurons are able to integrate into the olfactory circuitry and contribute to odor discrimination. We therefore hypothesized that perturbation of endogenous PTEN function may be beneficial for neuronal repair and post-injury recovery. To test this hypothesis, mice were treated with dichlobenil, a chemical shown to selectively destroy the olfactory sensory epithelium (Mombaerts et al., 1996; Yoon et al., 2005) in adult mice. In agreement with published reports, we observed a severe destruction of the main olfactory epithelium (MOE) neuronal layer in animals treated with dichlobenil when compared to controls (Supplementary Figure 7). Post dichlobenil treatment, all mice were evaluated weekly for their ability to detect novel odors (Odorant Habituation Test as described above). Consistent with previous report (Yoon et al., 2005), all drug treated mice, regardless of genotype, lost their ability to detect odorants 2 weeks after treatment (Figure 6B, top panel). However, $Pten^{loxp/loxp}$;$mGFAP$-Cre^+ mice showed an improvement in odorant detection 4 weeks post treatment (Figure 6B, middle panel). MOE examination after 4 weeks of dichlobenil treatment showed comparable regeneration of the epithelial layer in both control and mutant mice with no difference in Pten (Supplementary Figure 8B) or p-S6 (Supplementary Figure 8C) stainings, indicating improved behavioral test performance in the mutant animals is not due to enhanced regeneration or Pten deletion in mutant MOE. By 6 weeks post treatment, the $Pten^{loxp/loxp}$;$mGFAP$-Cre^+ mice had almost recovered to pre-treatment stage (Figure 6B, bottom panel). These results suggest $Pten$ null cells in the OB can establish normal connections with peripheral olfactory epithelium and enhanced NSC self-renewal and proliferation in $Pten$ deleted SEZ may help OB recovery from acute damage.

PTEN Deletion Enhances Post-Stroke Neuroblast Migration

Stroke is a common cause of neuronal damage. Seven to ten days after the initial insult, SEZ-born neuroblasts proliferate and migrate to the site of injury, contributing to post-stroke neurogenesis and recovery (Arvidsson et al., 2002; Jin et al., 2003; Parent, 2002; Tsai et al., 2006). We tested whether $Pten$ deletion in SEZ NSCs could enhance neuroblast proliferation and migration after ischemic injury. For this, we introduced a limited stroke in the sensorimotor cortex of the brain, which closely mimics the human condition and quantified the location and number of immature neurons with the protein marker doublecortin (DCX) (Carmichael, 2005; Ohab et al., 2006). As reported in normal adult mice (Ohab et al., 2006; Tsai et al., 2006), there were no DCX$^+$ cells in the cortex of either control or $Pten^{loxp/loxp}$;$mGFAP$-Cre^+ mice before stroke (data not shown), suggesting that $Pten$ null NSCs in the SEZ do not migrate to the cortex without additional stimulation (Supplementary Figure 9). Conditional $Pten$ deletion also had no effect on infarct size (Supplementary Figure 10A).

One week after stroke, DCX$^+$ cells were found in subcortical white matter and peri-infarct cortex of both groups (Figure 7A, left panels). However, $Pten^{loxp/loxp}$;$mGFAP$-Cre^+ mice showed a large and statistically significant increase of DCX$^+$ neuroblasts in the peri-infarct cortex at day 7 when compared to controls (Figure 7A, right panels, >4500 more immature neurons per animal in mutant vs. control; P<0.001), suggesting that $Pten$ null NSCs and their progenies can readily respond to ischemic injury and migrate to the damaged site. Staining of P-S6 marker further supports the idea that it is $Pten$ null neuroblasts which contribute to the

increased DCX$^+$ population in the peri-infarct site (Figure *7B*). These results indicate that PTEN is a potent negative regulator of NSC/progenitor proliferation and neurogenesis in response to injury.

Previous studies have shown that despite the migration of large numbers of newly born immature neurons to peri-infarct cortex in the first week after stroke, only a small percentage survive long term (Arvidsson et al., 2002; Ohab et al., 2006). To determine if PTEN plays a role in the long-term survival and differentiation of immature neurons in regions of damage after stroke, we labeled newly born cells in the first week after stroke with BrdU, and co-labeled these cells 90 days later with double staining for the mature neuronal marker NeuN. There was no difference in stereological counts of BrdU/NeuN cells between *Pten$^{loxp/loxp}$*;*mGFAP-Cre$^+$* mice and littermate controls 90 days after stroke (315 ± 123 vs. 303 ± 199 cells per animal in mutant and control $\pm$ SEM, respectively). This data indicate that though PTEN plays a prominent role in the control the initial proliferation and migration of immature neurons in post-stroke neurogenesis, it does not play an autonomous role in the survival of these cells in the long term.

DISCUSSION

Neurological disorders are the leading source of disability. Currently there are no treatments that promote repair and recovery in the brain from any major neurological disorder, including stroke, degenerative disease, and trauma. NSCs are cells that can give rise to the major components of the brain and spinal cord, thus attractive resources for repairing neurological disorders (Lindvall and Kokaia, 2006). The major challenges of NSC-mediated neuronal repair are 1) to understand the key pathways involved in controlling NSC self-renewal, proliferation, survival and differentiation, 2) to develop methodologies for manipulating these pathways towards therapeutic use, and 3) to test the potential benefit of NSCs and their progenies in human disease-relevant model systems before being used on human patients.

In this study we demonstrated that deletion of *Pten* in adult NSCs is not tumorigenic but promotes NSC expansion. Progeny from *Pten* null NSCs follow the endogenous migratory cues, differentiate, and integrate into the existing circuitry. Under conditions of acute damage, such as olfactory epithelium ablation, animals with *Pten* NSC deletion exhibited faster recovery. These data suggest that conditional manipulation of the PTEN/PI3K pathway in NSCs may be beneficial for NSC expansion, proliferation, and survival, in turn, promoting recovery and the integration of newly born neurons to existing or damaged neuronal networks associated with constitutive neurogenesis.

Stem cell self-renewal is known to be regulated by different signaling pathways, but the effect of a specific pathway may depend on the developmental stage or lineage of a stem cell population. For example, deletion of p21 in adult neural stem cells results in a transient increase in neurospheres formation with a subsequent decline in stem cell numbers; a phenomenon known as stem cell "exhaustion" (Kippin et al., 2005). Although, in a similar fashion, PTEN loss leads to the "exhaustion" of adult hematopoietic stem cells (Yilmaz et al., 2006; Zhang et al., 2006; and our unpublished observation), conditional deletion of *Pten* in both embryonic and adult NSC promotes a sustained self-renewal and stem/progenitor expansion (Groszer et al., 2006; Groszer et al., 2001; and this study). Significantly, we observed that the mutant cultures maintain an enhanced self-renewal, proliferation/survival rate, and neurogenic potential over extremely long-term expansion times under clonal conditions, suggesting that the role of PTEN in regulating stem cell activity may be modulated by factors specific to the neural stem cell lineage. Therefore, further study of these lineage- or developmental stage-specific mediators of self-renewal pathways will be increasingly critical for our understanding of the underlying mechanisms of stem cell self-renewal and therapeutic manipulations.

Our previous studies and those by others demonstrated that *Pten* deletion in the embryonic brain leads to abnormal histoarchitecture with severe layering defects (Backman et al., 2001; Groszer et al., 2001; Marino et al., 2002; Yue et al., 2005). However, as *Pten* deletion happens in nearly 100% of the neural stem/progenitor cells, it is unclear whether the abnormal phenotypes observed are caused by intrinsic migratory defects of *Pten*-null neurons, extrinsic microenvironmental cues provided by *Pten* null radial glia, or perhaps both (Groszer et al., 2001). In this study, we demonstrated that in the presence of wild-type environmental cues, *Pten* null adult NSCs and their progenies can follow the endogenous migration pathway, undergo differentiation, and reach their normal target. This result is consistent with a previous study on *Pten* heterozygous mice showing that $Pten^{+/-}$ cells migrated to the outer layers of the OB more rapidly and incorporated at the same sites as $Pten^{+/+}$ cells (Li et al., 2002). Therefore, the extrinsic microenvironment cues plays a more predominant role in controlling the migratory behavior of SEZ-derived *Pten* null NSCs and their progenies.

Nearly 90% of the GCs in the OB are SEZ-derived and incorporated postnatally, and their survival depends on incoming activities (Brunjes, 1994; Rosselli-Austin and Williams, 1990). GCs are also known to extensively shape mitral cell response to odors (Yokoi et al., 1995), and there is evidence that the OB circuitry maximizes differences in odor representations (Dulac, 2005; Friedrich and Laurent, 2001). Animals carrying a mutation in the cyclic nucleotide gated channel are not able to transduce the signal from the olfactory receptors in the olfactory neurons (Baker et al., 1999) and have smaller GCL volume and OB mass (Petreanu and Alvarez-Buylla, 2002). The lack of electrical activity in the OB of these mice dramatically reduced the survival of newly generated neurons of the GCL, suggesting that peripheral olfactory epithelium plays a critical role in the survival of GCL neurons in the OB (Petreanu and Alvarez-Buylla, 2002). Our results showed that PTEN loss in SEZ NSCs leads to an increase in GCL volume and OB size as well as an improvement in olfactory function, suggesting that the *Pten* null SEZ-derived GCL neurons are able to integrate into the existing circuitry, receive electrical input from olfactory epithelium and are thus functional. Because *Pten* conditional deletion in adult NSCs also enhances the recovery of olfactory function after ablation of olfactory epithelium, our data also suggest an important role for SEZ-derived neurons in reestablishment of the connection between OB and olfactory epithelium during acute damage via a currently unknown mechanism.

SEZ-born progenitors are known to play a role in post-ischemic injury recovery (Ohab et al., 2006). In a stroke-injury model, *Pten* conditional knockout animals showed a robust increase in cell proliferation and DCX[+] neuroblast migration from the SEZ over long distances to the peri-infarct cortex, suggesting *Pten* null neuroblasts are responsive to chemotactic stimulation and can migrate to the injury site. Although the SEZ DCX volume did not increase in PTEN conditional knockout mice post-stroke when compared to non-stroke animals (Supplementary Figure 10B), the significantly enhanced proliferation and migration of *Pten* null neuroblasts to the peri-infarct cortex suggested that *Pten* null neuroblasts are primed for the signals that induce post-stroke neurogenesis. *Pten* deletion might have been expected to promote neuroblast survival as it potentiates the action of the PI3K/Akt pathway, a common downstream signaling pathway for many of the neural stem cell survival and differentiation growth factors (Greenberg and Jin, 2006). Interestingly, *Pten* conditional deletion in these neuroblasts is not sufficient to promote their long-term differentiation/survival and functional integration once they have migrated into peri-infarct cortex. Thus, in addition to soluble growth factor signaling, the cellular environment of the peri-infarct cortex may exert an important degree of control over cell survival in newly born neurons after stroke.

Stem cell-based therapies, including the promotion of endogenous neurogenesis or transplantation of stem/progenitor cells, are limited in large part by the death of the progenitor pool (Goldman, 2005). In post-stroke neurogenesis, despite a robust generation of newly born

neurons, ninety percent of them eventually die (Ohab et al., 2006). After stem/progenitor transplantation, a similar result is seen in which most transplanted cells die or fail to differentiate. The differential roles of PTEN defined in the present study highlight the key differences between constitutive/normal and injury-induced neurogenesis. PTEN inactivation alone is sufficient to promote a significant increase in neurogenesis, neuronal survival and improved function in the olfactory bulb but insufficient to promote long-term survival after stroke. Though both post-stroke and normal neurogenesis involve growth factor signaling within glial and vascular niches (Hagg, 2007; Nilsson et al., 1999; Ohab et al., 2006; Puche and Baker, 2007; Teramoto et al., 2003) post-stroke neurogenesis requires additional, likely, cellular signals that are independent of the common PI3K-AKT-mediated growth factor signaling pathway. In designing successful stem cell based therapies it will be important to determine both the molecular and cellular constituents that support survival and differentiation of stem cell progenies.

Supplementary Material

Refer to Web version on PubMed Central for supplementary material.

Acknowledgements

REFERENCES

Arvidsson A, Collin T, Kirik D, Kokaia Z, Lindvall O. Neuronal replacement from endogenous precursors in the adult brain after stroke. Nat Med 2002;8:963–970. [PubMed: 12161747]

Backman SA, Stambolic V, Suzuki A, Haight J, Elia A, Pretorius J, Tsao MS, Shannon P, Bolon B, Ivy GO, Mak TW. Deletion of Pten in mouse brain causes seizures, ataxia and defects in soma size resembling Lhermitte-Duclos disease. Nat Genet 2001;29:396–403. [PubMed: 11726926]

Baker H, Cummings DM, Munger SD, Margolis JW, Franzen L, Reed RR, Margolis FL. Targeted deletion of a cyclic nucleotide-gated channel subunit (OCNC1): biochemical and morphological consequences in adult mice. J Neurosci 1999;19:9313–9321. [PubMed: 10531436]

Brunjes PC. Unilateral naris closure and olfactory system development. Brain Res Brain Res Rev 1994;19:146–160. [PubMed: 8167658]

Bush TG, Savidge TC, Freeman TC, Cox HJ, Campbell EA, Mucke L, Johnson MH, Sofroniew MV. Fulminant jejuno-ileitis following ablation of enteric glia in adult transgenic mice. Cell 1998;93:189–201. [PubMed: 9568712]

Carmichael ST. Rodent models of focal stroke: size, mechanism, and purpose. NeuroRx 2005;2:396–409. [PubMed: 16389304]

Cecchi GA, Petreanu LT, Alvarez-Buylla A, Magnasco MO. Unsupervised learning and adaptation in a model of adult neurogenesis. J Comput Neurosci 2001;11:175–182. [PubMed: 11717533]

Curtis MA, Kam M, Nannmark U, Anderson MF, Axell MZ, Wikkelso C, Holtas S, van Roon-Mom WM, Bjork-Eriksson T, Nordborg C, et al. Human neuroblasts migrate to the olfactory bulb via a lateral ventricular extension. Science 2007;315:1243–1249. [PubMed: 17303719]

Datta SR, Brunet A, Greenberg ME. Cellular survival: a play in three Akts. Genes Dev 1999;13:2905–2927. [PubMed: 10579998]

Doetsch F. The glial identity of neural stem cells. Nat Neurosci 2003;6:1127–1134. [PubMed: 14583753]

Doetsch F, Alvarez-Buylla A. Network of tangential pathways for neuronal migration in adult mammalian brain. Proc Natl Acad Sci U S A 1996;93:14895–14900. [PubMed: 8962152]

Doetsch F, Caille I, Lim DA, Garcia-Verdugo JM, Alvarez-Buylla A. Subventricular zone astrocytes are neural stem cells in the adult mammalian brain. Cell 1999;97:703–716. [PubMed: 10380923]

Dulac C. Molecular architecture of pheromone sensing in mammals. Novartis Found Symp 2005;268:100–107. [PubMed: 16206877]discussion 107–110, 167–170.

Emsley JG, Mitchell BD, Kempermann G, Macklis JD. Adult neurogenesis and repair of the adult CNS with neural progenitors, precursors, and stem cells. Prog Neurobiol 2005;75:321–341. [PubMed: 15913880]

Enwere E, Shingo T, Gregg C, Fujikawa H, Ohta S, Weiss S. Aging results in reduced epidermal growth factor receptor signaling, diminished olfactory neurogenesis, and deficits in fine olfactory discrimination. J Neurosci 2004;24:8354–8365. [PubMed: 15385618]

Feng Y, Walsh CA. Protein-protein interactions, cytoskeletal regulation and neuronal migration. Nat Rev Neurosci 2001;2:408–416. [PubMed: 11389474]

Fiske BK, Brunjes PC. Cell death in the developing and sensory-deprived rat olfactory bulb. J Comp Neurol 2001;431:311–319. [PubMed: 11170007]

Fraser MM, Zhu X, Kwon CH, Uhlmann EJ, Gutmann DH, Baker SJ. Pten loss causes hypertrophy and increased proliferation of astrocytes in vivo. Cancer Res 2004;64:7773–7779. [PubMed: 15520182]

Friedrich RW, Laurent G. Dynamic optimization of odor representations by slow temporal patterning of mitral cell activity. Science 2001;291:889–894. [PubMed: 11157170]

Funamoto S, Meili R, Lee S, Parry L, Firtel RA. Spatial and temporal regulation of 3-phosphoinositides by PI 3-kinase and PTEN mediates chemotaxis. Cell 2002;109:611–623. [PubMed: 12062104]

Garcia AD, Doan NB, Imura T, Bush TG, Sofroniew MV. GFAP-expressing progenitors are the principal source of constitutive neurogenesis in adult mouse forebrain. Nat Neurosci 2004;7:1233–1241. [PubMed: 15494728]

Gheusi G, Cremer H, McLean H, Chazal G, Vincent JD, Lledo PM. Importance of newly generated neurons in the adult olfactory bulb for odor discrimination. Proc Natl Acad Sci U S A 2000;97:1823–1828. [PubMed: 10677540]

Goldman S. Stem and progenitor cell-based therapy of the human central nervous system. Nat Biotechnol 2005;23:862–871. [PubMed: 16003375]

Goldman SA. Adult neurogenesis: from canaries to the clinic. J Neurobiol 1998;36:267–286. [PubMed: 9712309]

Greenberg DA, Jin K. Growth factors and stroke. NeuroRx 2006;3:458–465. [PubMed: 17012059]

Groszer M, Erickson R, Scripture-Adams DD, Dougherty JD, Le Belle J, Zack JA, Geschwind DH, Liu X, Kornblum HI, Wu H. PTEN negatively regulates neural stem cell self-renewal by modulating G0-G1 cell cycle entry. Proc Natl Acad Sci U S A 2006;103:111–116. [PubMed: 16373498]

Groszer M, Erickson R, Scripture-Adams DD, Lesche R, Trumpp A, Zack JA, Kornblum HI, Liu X, Wu H. Negative regulation of neural stem/progenitor cell proliferation by the Pten tumor suppressor gene in vivo. Science 2001;294:2186–2189. [PubMed: 11691952]

Hack MA, Saghatelyan A, de Chevigny A, Pfeifer A, Ashery-Padan R, Lledo PM, Gotz M. Neuronal fate determinants of adult olfactory bulb neurogenesis. Nat Neurosci 2005;8:865–872. [PubMed: 15951811]

Hagg T. Endogenous regulators of adult CNS neurogenesis. Curr Pharm Des 2007;13:1829–1840. [PubMed: 17584112]

Iijima M, Devreotes P. Tumor suppressor PTEN mediates sensing of chemoattractant gradients. Cell 2002;109:599–610. [PubMed: 12062103]

Imura T, Kornblum HI, Sofroniew MV. The predominant neural stem cell isolated from postnatal and adult forebrain but not early embryonic forebrain expresses GFAP. J Neurosci 2003;23:2824–2832. [PubMed: 12684469]

Jin K, Sun Y, Xie L, Peel A, Mao XO, Batteur S, Greenberg DA. Directed migration of neuronal precursors into the ischemic cerebral cortex and striatum. Mol Cell Neurosci 2003;24:171–189. [PubMed: 14550778]

Kippin TE, Martens DJ, van der Kooy D. p21 loss compromises the relative quiescence of forebrain stem cell proliferation leading to exhaustion of their proliferation capacity. Genes Dev 2005;19:756–767. [PubMed: 15769947]

Kwon CH, Zhu X, Zhang J, Knoop LL, Tharp R, Smeyne RJ, Eberhart CG, Burger PC, Baker SJ. Pten regulates neuronal soma size: a mouse model of Lhermitte-Duclos disease. Nat Genet 2001;29:404–411. [PubMed: 11726927]

Lagace DC, Whitman MC, Noonan MA, Ables JL, DeCarolis NA, Arguello AA, Donovan MH, Fischer SJ, Farnbauch LA, Beech RD, DiLeone RJ, Greer CA, Mandyam CD, Eisch AJ. Dynamic contribution of nestin-expressing stem cells to adult neurogenesis. J Neurosci 2007;27:12623–12629. [PubMed: 18003841]

Lee JO, Yang H, Georgescu MM, Di Cristofano A, Maehama T, Shi Y, Dixon JE, Pandolfi P, Pavletich NP. Crystal structure of the PTEN tumor suppressor: implications for its phosphoinositide phosphatase activity and membrane association. Cell 1999;99:323–334. [PubMed: 10555148]

Lesche R, Groszer M, Gao J, Wang Y, Messing A, Sun H, Liu X, Wu H. Cre/loxP-mediated inactivation of the murine Pten tumor suppressor gene. Genesis 2002;32:148–149. [PubMed: 11857804]

Li J, Simpson L, Takahashi M, Miliaresis C, Myers MP, Tonks N, Parsons R. The PTEN/MMAC1 tumor suppressor induces cell death that is rescued by the AKT/protein kinase B oncogene. Cancer Res 1998;58:5667–5672. [PubMed: 9865719]

Li L, Liu F, Salmonsen RA, Turner TK, Litofsky NS, Di Cristofano A, Pandolfi PP, Jones SN, Recht LD, Ross AH. PTEN in neural precursor cells: regulation of migration, apoptosis, and proliferation. Mol Cell Neurosci 2002;20:21–29. [PubMed: 12056837]

Liaw D, Marsh DJ, Li J, Dahia PL, Wang SI, Zheng Z, Bose S, Call KM, Tsou HC, Peacocke M, et al. Germline mutations of the PTEN gene in Cowden disease, an inherited breast and thyroid cancer syndrome. Nat Genet 1997;16:64–67. [PubMed: 9140396]

Liliental J, Moon SY, Lesche R, Mamillapalli R, Li D, Zheng Y, Sun H, Wu H. Genetic deletion of the Pten tumor suppressor gene promotes cell motility by activation of Rac1 and Cdc42 GTPases. Curr Biol 2000;10:401–404. [PubMed: 10753747]

Lindvall O, Kokaia Z. Stem cells for the treatment of neurological disorders. Nature 2006;441:1094–1096. [PubMed: 16810245]

Lledo PM, Alonso M, Grubb MS. Adult neurogenesis and functional plasticity in neuronal circuits. Nat Rev Neurosci 2006;7:179–193. [PubMed: 16495940]

Lois C, Garcia-Verdugo JM, Alvarez-Buylla A. Chain migration of neuronal precursors. Science 1996;271:978–981. [PubMed: 8584933]

Luskin MB. Restricted proliferation and migration of postnatally generated neurons derived from the forebrain subventricular zone. Neuron 1993;11:173–189. [PubMed: 8338665]

Maehama T, Taylor GS, Dixon JE. PTEN AND MYOTUBULARIN: Novel Phosphoinositide Phosphatases. Annu Rev Biochem 2001;70:247–279. [PubMed: 11395408]

Marino S, Krimpenfort P, Leung C, van der Korput HA, Trapman J, Camenisch I, Berns A, Brandner S. PTEN is essential for cell migration but not for fate determination and tumourigenesis in the cerebellum. Development 2002;129:3513–3522. [PubMed: 12091320]

Mombaerts P, Wang F, Dulac C, Chao SK, Nemes A, Mendelsohn M, Edmondson J, Axel R. Visualizing an olfactory sensory map. Cell 1996;87:675–686. [PubMed: 8929536]

Najbauer J, Leon M. Olfactory experience modulated apoptosis in the developing olfactory bulb. Brain Res 1995;674:245–251. [PubMed: 7796103]

Nelen MR, van Staveren WC, Peeters EA, Hassel MB, Gorlin RJ, Hamm H, Lindboe CF, Fryns JP, Sijmons RH, Woods DG, et al. Germline mutations in the PTEN/MMAC1 gene in patients with Cowden disease. Hum Mol Genet 1997;6:1383–1387. [PubMed: 9259288]

Nilsson M, Perfilieva E, Johansson U, Orwar O, Eriksson PS. Enriched environment increases neurogenesis in the adult rat dentate gyrus and improves spatial memory. J Neurobiol 1999;39:569–578. [PubMed: 10380078]

Ohab JJ, Fleming S, Blesch A, Carmichael ST. A neurovascular niche for neurogenesis after stroke. J Neurosci 2006;26:13007–13016. [PubMed: 17167090]

Parent JM. The role of seizure-induced neurogenesis in epileptogenesis and brain repair. Epilepsy Res 2002;50:179–189. [PubMed: 12151127]

Peterson DA. Stem cells in brain plasticity and repair. Curr Opin Pharmacol 2002;2:34–42. [PubMed: 11786306]
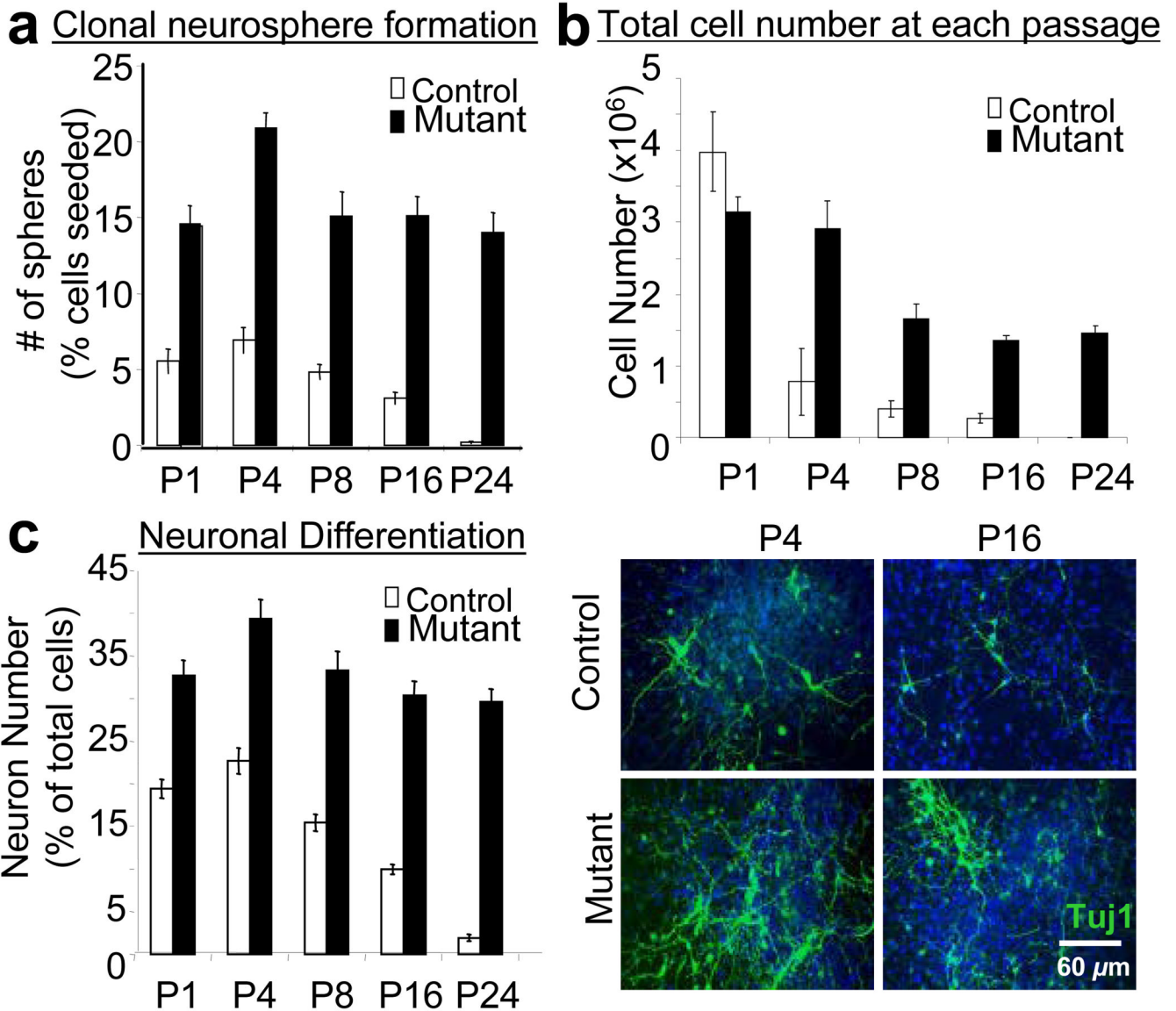
Petreanu L, Alvarez-Buylla A. Maturation and death of adult-born olfactory bulb granule neurons: role of olfaction. J Neurosci 2002;22:6106–6113. [PubMed: 12122071]

Pomeroy SL, LaMantia AS, Purves D. Postnatal construction of neural circuitry in the mouse olfactory bulb. J Neurosci 1990;10:1952–1966. [PubMed: 2355260]

Puche AC, Baker H. Olfactory cell derivation and migration. J Mol Histol 2007;38:513–515. [PubMed: 17879131]

Raftopoulou M, Etienne-Manneville S, Self A, Nicholls S, Hall A. Regulation of cell migration by the C2 domain of the tumor suppressor PTEN. Science 2004;303:1179–1181. [PubMed: 14976311]

Rochefort C, Gheusi G, Vincent JD, Lledo PM. Enriched odor exposure increases the number of newborn neurons in the adult olfactory bulb and improves odor memory. J Neurosci 2002;22:2679–2689. [PubMed: 11923433]

Rosselli-Austin L, Williams J. Enriched neonatal odor exposure leads to increased numbers of olfactory bulb mitral and granule cells. Brain Res Dev Brain Res 1990;51:135–137.

Shors TJ, Miesegaes G, Beylin A, Zhao M, Rydel T, Gould E. Neurogenesis in the adult is involved in the formation of trace memories. Nature 2001;410:372–376. [PubMed: 11268214]

Soriano P. Generalized lacZ expression with the ROSA26 Cre reporter strain. Nat Genet 1999;21:70–71. [PubMed: 9916792]

Stiles B, Groszer M, Wang S, Jiao J, Wu H. PTENless means more. Dev Biol 2004;273:175–184. [PubMed: 15328005]

Tamura M, Gu J, Matsumoto K, Aota S, Parsons R, Yamada KM. Inhibition of cell migration, spreading, and focal adhesions by tumor suppressor PTEN. Science 1998;280:1614–1617. [PubMed: 9616126]

Teramoto T, Qiu J, Plumier JC, Moskowitz MA. EGF amplifies the replacement of parvalbumin-expressing striatal interneurons after ischemia. J Clin Invest 2003;111:1125–1132. [PubMed: 12697732]

Trinh K, Storm DR. Detection of odorants through the main olfactory epithelium and vomeronasal organ of mice. Nutr Rev 2004;62:S189–S192. [PubMed: 15630934]discussion S224-141.

Tsai PT, Ohab JJ, Kertesz N, Groszer M, Matter C, Gao J, Liu X, Wu H, Carmichael ST. A critical role of erythropoietin receptor in neurogenesis and post-stroke recovery. J Neurosci 2006;26:1269–1274. [PubMed: 16436614]

Vivanco I, Sawyers CL. The phosphatidylinositol 3-Kinase AKT pathway in human cancer. Nat Rev Cancer 2002;2:489–501. [PubMed: 12094235]

Winner B, Cooper-Kuhn CM, Aigner R, Winkler J, Kuhn HG. Long-term survival and cell death of newly generated neurons in the adult rat olfactory bulb. Eur J Neurosci 2002;16:1681–1689. [PubMed: 12431220]

Yamashita T, Ninomiya M, Hernandez Acosta P, Garcia-Verdugo JM, Sunabori T, Sakaguchi M, Adachi K, Kojima T, Hirota Y, Kawase T, et al. Subventricular zone-derived neuroblasts migrate and differentiate into mature neurons in the post-stroke adult striatum. J Neurosci 2006;26:6627–6636. [PubMed: 16775151]

Yokoi M, Mori K, Nakanishi S. Refinement of odor molecule tuning by dendrodendritic synaptic inhibition in the olfactory bulb. Proc Natl Acad Sci U S A 1995;92:3371–3375. [PubMed: 7724568]

Yoon H, Enquist LW, Dulac C. Olfactory inputs to hypothalamic neurons controlling reproduction and fertility. Cell 2005;123:669–682. [PubMed: 16290037]

Yue Q, Groszer M, Gil JS, Berk AJ, Messing A, Wu H, Liu X. PTEN deletion in Bergmann glia leads to premature differentiation and affects laminar organization. Development 2005;132:3281–3291. [PubMed: 15944184]
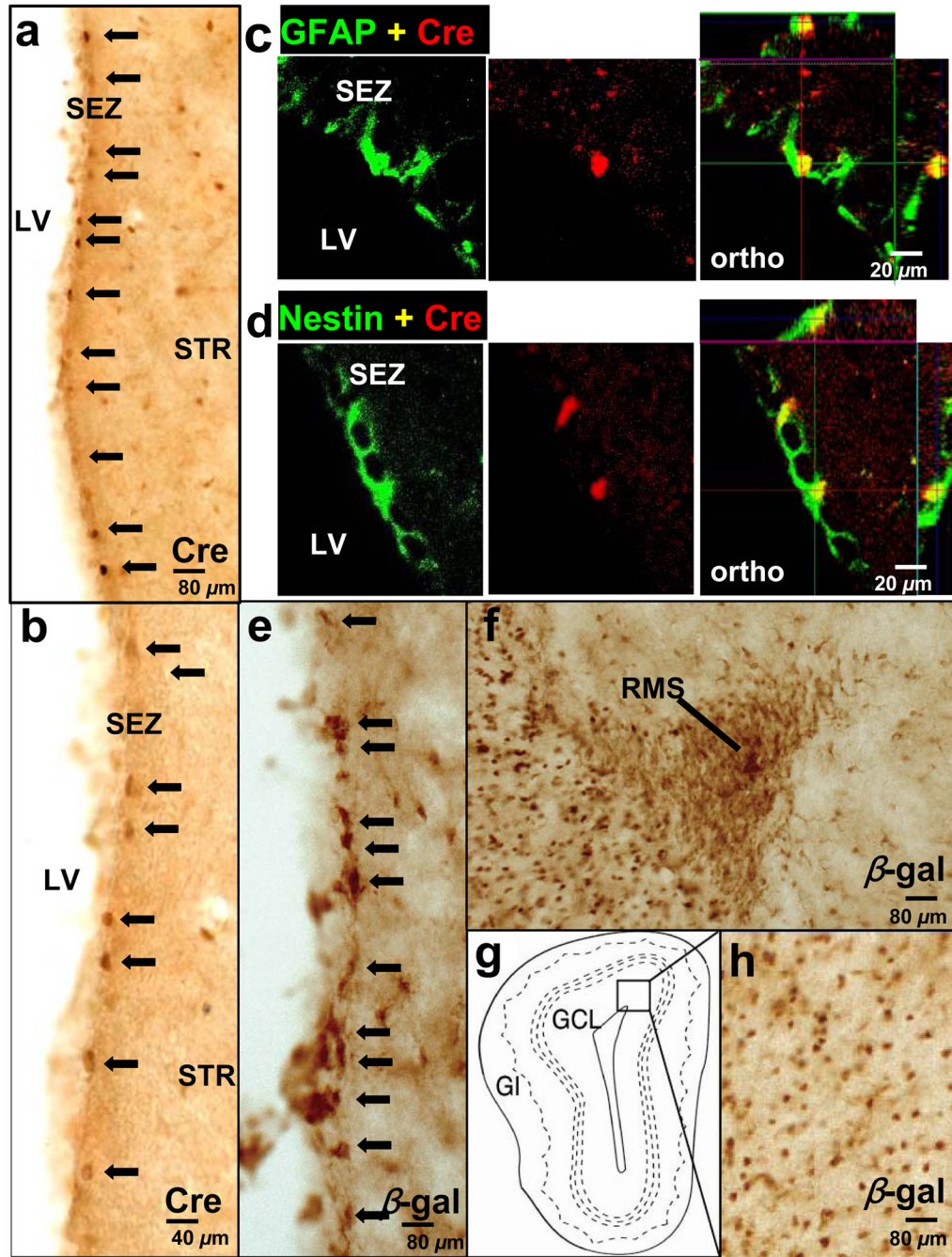
Figure 1. *mGFAP-Cre* line for conditionally targeting adult neural stem/progenitor cells
(A,B,E,F,H) Survey images of coronal sections of the SEZ (A,B,E), RMS (F), and OB (H) stained by bright-field immunohistochemistry. A small number of cells in the SEZ express Cre (A, low mag; B, high mag). (C,D) Confocal micrographs of single optical slices through cells in the SEZ that are double stained by immunofluorescence for Cre and GFAP (C) or Cre and Nestin (D). Individual channels and orthogonal analysis show that all Cre-expressing cells in the SEZ also express Nestin (C) and GFAP (D). Orthogonal images (ortho) show three-dimensional analysis of individual cells at specific sites marked by intersecting *x, y*, and *z* axes. Many cells express the reporter protein β-gal (E) in the neurogenic proliferative regions of the SEZ. Migrating neuroblasts in the RMS (F) and granule neurons in the OB (H) also express

β-gal. Box in G indicates the region shown in H. Arrows in A, B, and E indicate representative Cre or β-gal-positive cells in SEZ. SEZ, subependmyal zone; LV, left ventricle; STR, striatum; RMS, rostral migratory stream; OB, olfactory bulb; GCL, Granule Cell Layer; Gl, Glomeruli.

a Clonal neurosphere formation

b Total cell number at each passage

c Neuronal Differentiation

P4   P16

Figure 2. *Pten* deletion in clonal neurosphere cultures enhances stem cell self-renewal and neurogenesis over long-term serial clonal passages compared to the gradual senescence and decreased neurogenesis in wild-type cultures

(A) Neurosphere cultures generated from the adult SVZ of PTEN knockout (Mutant) and wild-type (Control) mice were cultured at clonal density (1000 cells/ml), passaged and re-seeded at clonal density every 2 weeks. Clonal neurosphere numbers, representative of the number of stem cells present in the culture, were significantly higher in mutant cultures at all passages (P<0.001). (B) The clonal neurospheres were then dissociated and the total cell number was counted at each passage followed by re-culturing at clonal density. After the first passage, mutant cultures consistently produced higher total cell numbers even after long-term serial clonal passaging whilst control cultures produced decreased cell numbers with time, eventually senescing by passage 24. Data are means ± SEM; *n* = 4. (C) In addition, the clonal neurospheres from mutant mice maintained their robust neurogenesis even at late clonal passages whilst the ability to generate neurons was dramatically attenuated in control cultures over time.

Immunocytochemistry for TUJ1+ cells (green) and the counterstain Hoescht (blue) are shown at passage 4 and 16. $n = 4$.
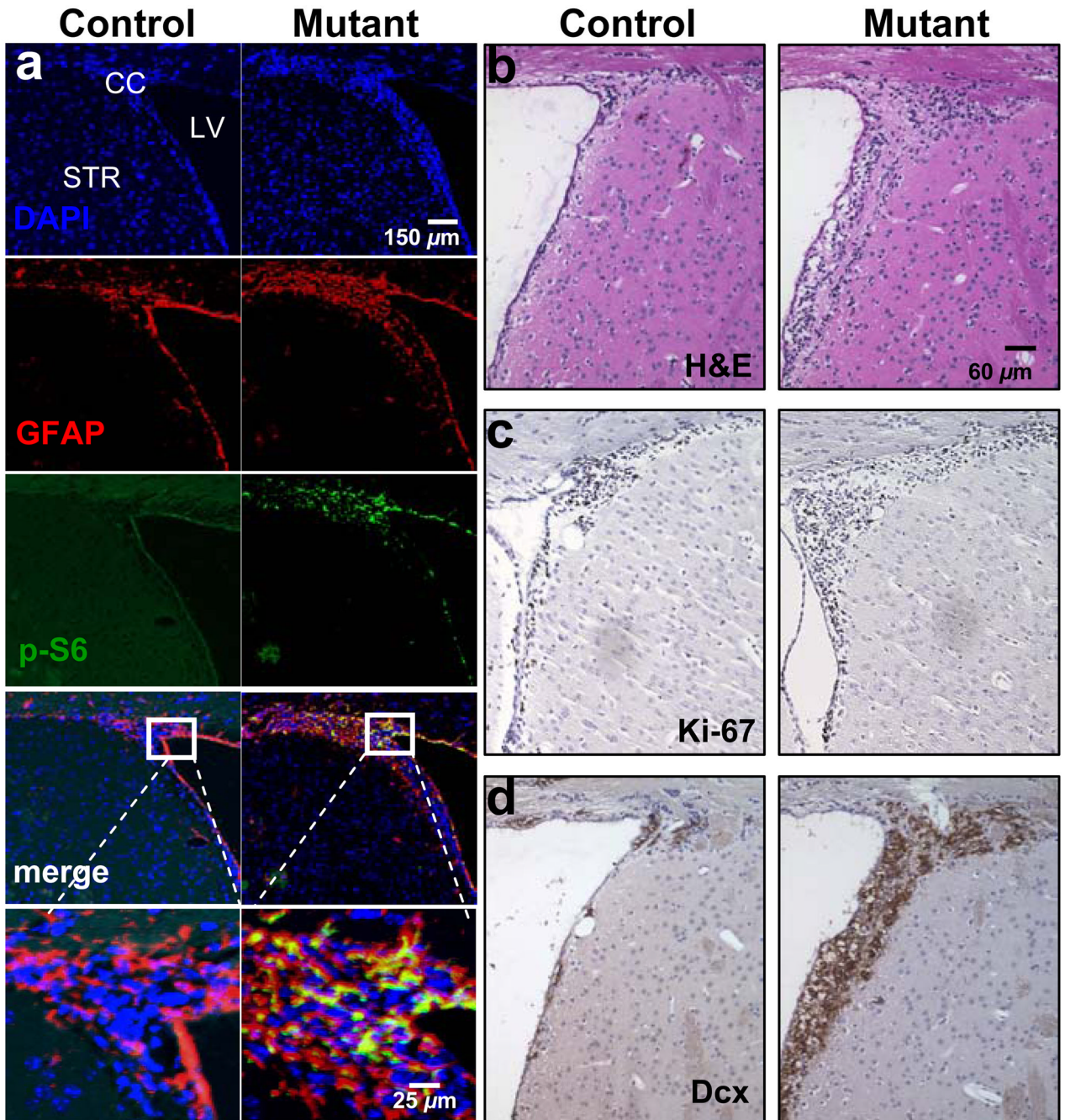
Figure 3. *mGFAP-Cre*-mediated *Pten* deletion lead s to expansion of adult neural stem cells and their progenies *in vivo*

Survey images of coronal sections of control and mutant SEZ. (A) Compared with littermate controls, mutant mice showed increased GFAP- and P-S6-positive labeled cells which co-localized in the SEZ. Images and graphs quantifying SEZ volume (B), Ki-67 counts (C), and DCX volume (D) demonstrate increased proliferation in mutant SEZ as compared to control regions. DAPI counter stain is used to visualize nuclei. Data are means ± SEM, *n* = 5. LV, lateral ventricle; CC, corpus collosum; STR, striatum; SEZ, subependymal zone; DCX, doublecortin.
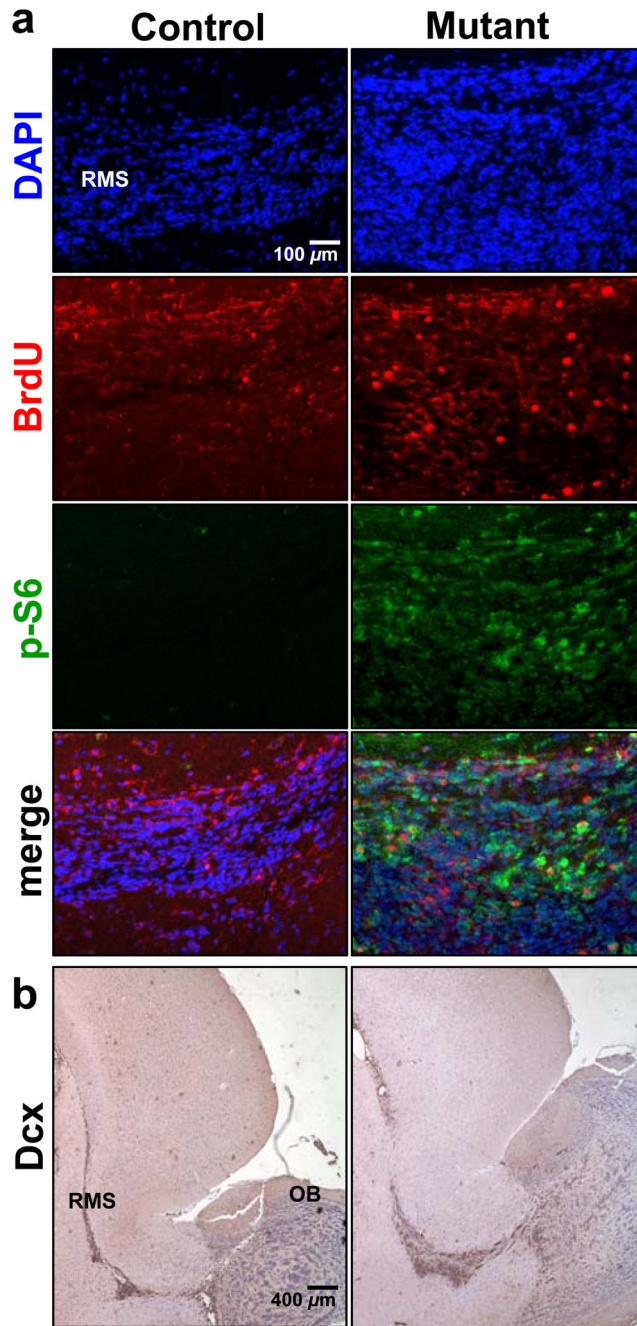
Figure 4. *Pten* deletion leads to enhanced migration of SEZ-born progenitors in RMS
(A) Quantification of BrdU$^+$ cells in RMS revealed an increase in *Pten* null SEZ-born progenitors migrating in the RMS when compared to control. (B) Representative images of RMS stained for BrdU, P-S6, and their colocalization shows the BrdU$^+$ population in mutant RMS is *Pten* null. (C and D) Survey images of sagittal sections of control and mutant RMS stained with DCX (C) and graph quantifying DCX$^+$ cells show an increase in the number of migrating neuroblasts in mutant RMS compared to control (D). Inserts show higher magnification of boxed area. (E) Quantification of the percentage of DCX$^+$ cells diverging from RMS pathway shows no difference between control and mutant. DAPI counter stain is

used to visualize nuclei. Data are means ± SEM, $n = 6$. RMS, rostral migratory stream; DCX, doublecortin; BrdU, 5-Bromo-2′-Deoxyuridine.
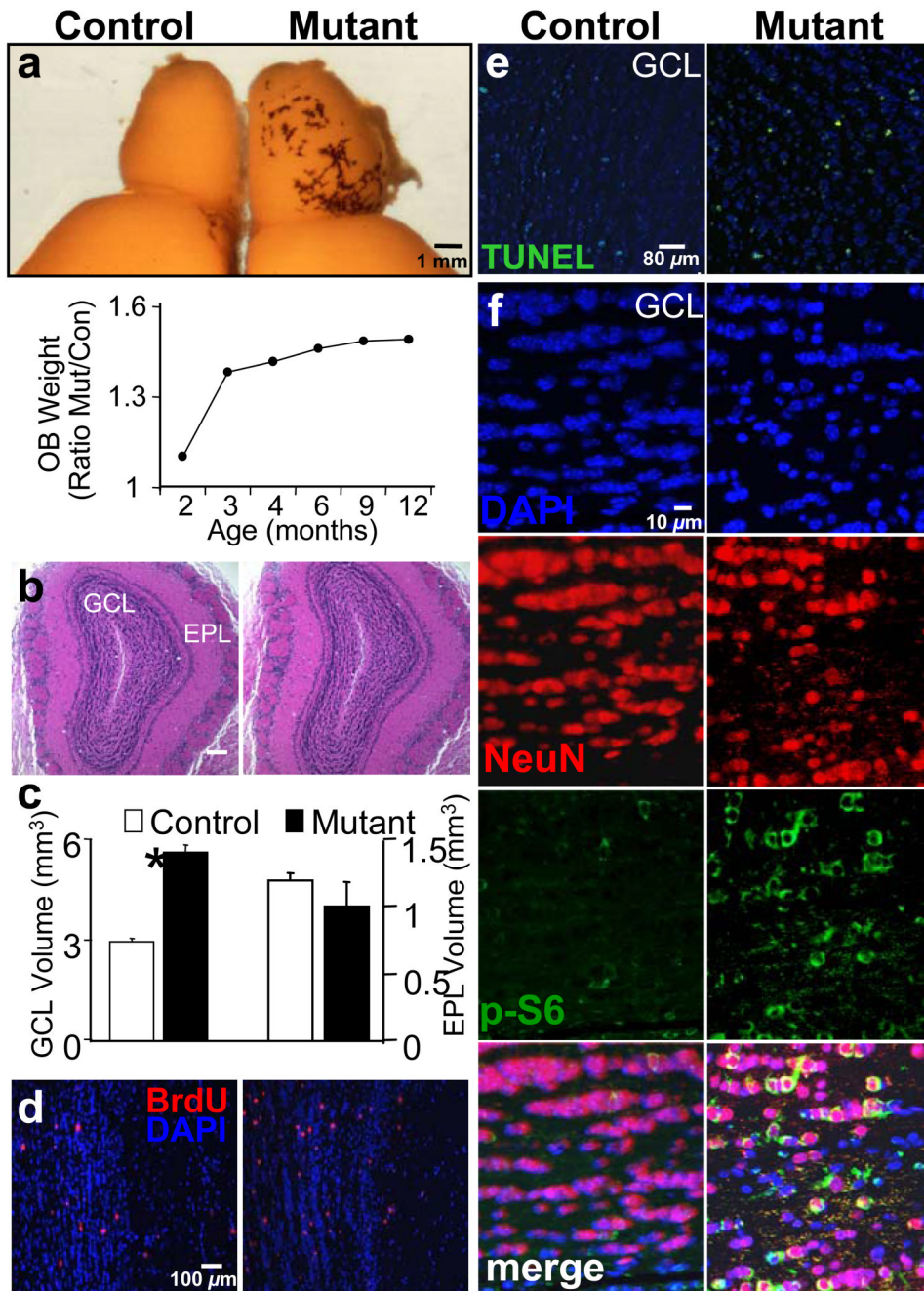
Figure 5. Increased OB mass and enhanced proliferation and migration of SEZ-born progenitors to the GCL of OB in mutant mice

(A) Enlarged OB of mutant mice. Photo shows a brain hemisphere from control and mutant mouse. Panel on right depicts the progressive increase in the ratio of mutant/control OB weight. $n = 40$. (B) Histological analysis of OB section from control and mutant mice reveals normal histoarchitecture. (C) GCL volume is increased in mutant mice whereas no significant change is observed in EPL. $n = 10$. (D) SEZ-born neuroblast migration was analyzed by BrdU pulse-labeling. Mice were injected with 200 mg/kg BrdU peritoneally, and distribution of BrdU-labeled cells was determined 2 weeks after injection. An increased number of BrdU-labeled cells were seen within the GCL. Quantification of BrdU-labeled cells within GCL indicates

Pten mutant mice had a significant increase in cell number at 2 weeks post injection. $n = 5$. (E) Using the TUNEL assay, we observed a significant decrease in the percentage of dying cells in the GCL of mutant animals as compared with control. $n = 5$. (F) Representative GCL images show enhanced immunoreactivity for NeuN and increased NeuN/P-S6 double positive cells in mutant when compared to a matched control region. Data are means ± SEM. OB, olfactory bulb; GCL, granule cell layer; EPL, external plexiform layer; BrdU, 5-Bromo-2′-Deoxyuridine; DAPI is used as counterstain to visualize nuclei.
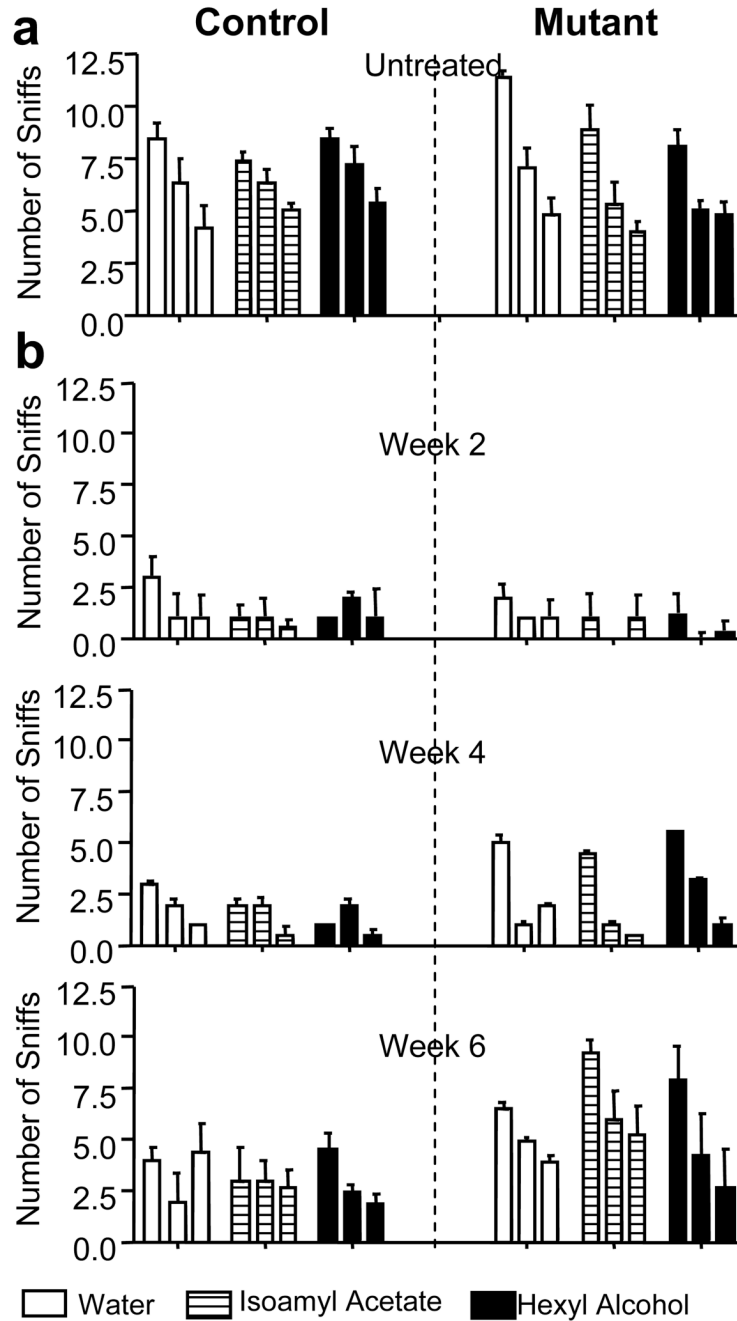
Figure 6. Enhanced olfactory habituation and recovery after epithelium injury in
$Pten^{loxp/loxp}$;mGFAP-Cre$^+$ **mice**
Control and mutant mice were subjected to the olfactory habituation test. Pre-training of wild-
type control mice to a cotton swab soaked in water habituated mice to the presence of the swab
in their cage. This was manifested as a decline in the number of sniffs with subsequent
exposures to the swab. During odorant testing, the cotton swab was laced with 50 µM isoamyl
acetate or 50 µM hexyl alcohol and introduced on three successive trials. The fact that the
control mice sniffed the isoamyl acetate- and hexyl alcohol-laced cotton swabs more times
than during the third exposure to the water swab indicated that the animal was able to smell
these odorants. (A) Compared to control, mutant mice sniffed the swabs less frequently in the

second and third exposures (all three conditions) signifying they habituated to the novel odorant faster than the control. $n = 14$ (control) and 12 (mutant). (B) Both control and mutant mice lost their ability to detect odorants at 2 weeks post treatment (top), whereas the ability of mutant mice to detect odorants began recovering at 4 weeks post treatment (middle), and their ability to detect odorants was restored to pre-treatment levels by week 6 (bottom). Data are means ± SEM; $n = 8$.
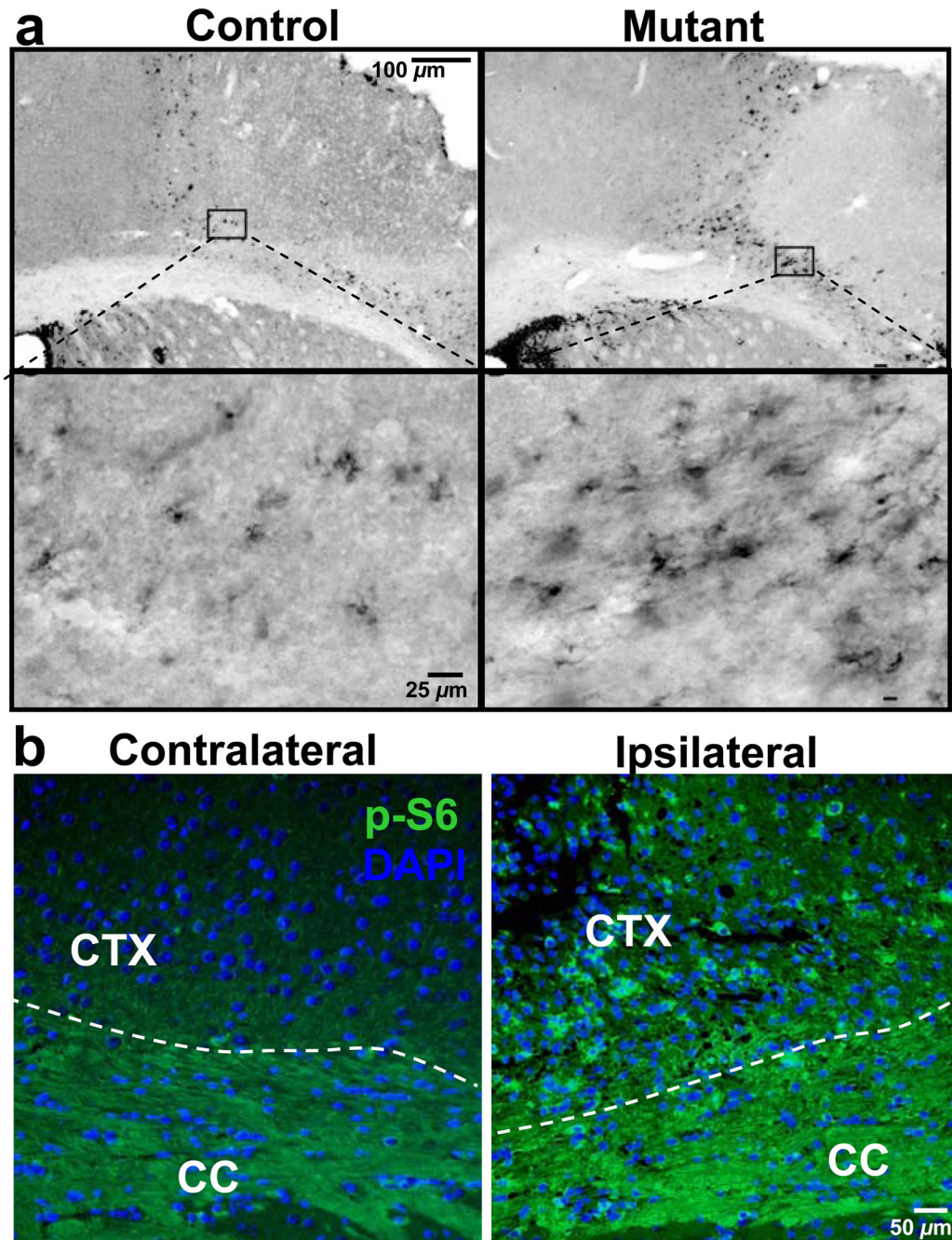
Figure 7. PTEN deletion enhances post-stroke neuroblast migration
(A) Quantification of DCX labeling in peri-infarct cortex and SEZ. DCX+ cells in control and mutant 7 d after stroke. Right panel shows stereological quantification of DCX+ cells in peri-infarct cortex. Scale bars: top, 100 µm; bottom, 25 µm. Data are means ± SEM; n = 6. (B) Representative images of p-S6 staining from both hemispheres of mutant mouse. Left panel shows hemisphere containing peri-infarct cortex which has increased staining for p-S6 in peri-infarct cortex when compared to uninjured cortex in the same animal (right panel).